Korea-Australia Rheology Journal
Vol. 18, No. 2, June 2006 pp. 91-98

# Comparison of interpretation methods for large amplitude oscillatory shear response

**Hyungsup Kim, Kyu Hyun[1], Dae-Jin Kim[2] and Kwang Soo Cho[3]***

*Department of Textile Engineering, Konkuk University, 1 Hwayang-dong, Kwangjin-Gu, Seoul 143-701, Korea*
*[1]School of Chemical and Biological Engineering, Seoul National University, San 56-1 Sinlim-dong, Kwanak-gu, Seoul 151-744, Korea*
*[2]Center for Academic Links to Industry for Collaborative Evolution, Kyungpook National University, 1370 Sangyeok-dong, Buk-gu, Daegu 702-701, Korea*
*[3]Department of Polymer Science, Kyungpook National University, 1370 Sangyeok-dong, Buk-gu, Daegu 702-701, Korea*

(Received April 3, 2006; final revision received May 15, 2006)

## Abstract

We compare FT (Fourier Transform) and SD (Stress Decomposition), the interpretation methods for LAOS (Large Amplitude Oscillatory Shear). Although the two methods are equivalent in mathematics, they are significantly different in numerical procedures. Precision of FT greatly depends on sampling rate and length of data because FT of experimental data is the discrete version of Fourier integral theorem. FT inevitably involves unnecessary frequencies which must not appear in LAOS. On the other hand, SD is free from the problems from which FT suffers, because SD involves only odd harmonics of primary frequency. SD is based on two axioms on shear stress: [1] shear stress is a sufficiently smooth function of strain and its time derivatives; [2] shear stress satisfies macroscopic time-reversal symmetry. In this paper, we compared numerical aspects of the two interpretation methods for LAOS.

***Keywords*** : LAOS, Fourier transform, nonlinear viscoelasticity

## 1. Introduction

Oscillatory shear flow is very useful for identifying viscoelastic properties of complex fluids. Since linear viscoelasticity is based on concrete theoretical foundation, it is not difficult to extract useful information from the measurement under small amplitude oscillatory shear flow. When the strain amplitude is as large as the level that linear viscoelasticity is no longer valid, the shear stress as a function of time becomes distorted and deviate from a sinusoidal wave. Thus we cannot understand the nonlinear data from the view point of linear viscoelastic theory. Several researchers tried to develop a new method for interpreting the nonlinear wave form of stress.

One is to investigate stress shape itself, for example, stress curve as a function of time or stress as a function of strain (Lissajous pattern). This approach has already been presented by early researchers of LAOS; e.g., Philipoff (1966), Onogi *et al.* (1970), Krieger and Niu (1973), and Giacomin and Dealy (1993). The other is the Fourier transformation (FT) method. The nonlinear stress can be expanded as Fourier series with odd higher harmonics. FT method is sensitive enough to detect a small distortion of the stress signal compared with Lissajous figure. Even though this sensitivity is advantage of FT method, on the contrary, FT method is affected by the noise of stress signal. Thus Dusschoten and Wilhelm (2001) suggested the method of "increasing torque transducer sensitivity via oversampling".

It is noteworthy that FT inherently deals with frequencies that are not integer-multiples of the primary frequency. Effects of such frequency cannot appear in the theory of LAOS. The mathematics of FT guarantees that the effects of such frequencies are cancelled and those of only odd harmonics survive. However, the cancellation is not complete because experiment always includes considerable errors and because the discrete FT has inherent deviation from continuous FT due to discretization. Numerical FT of experimental data becomes better as longer series of data are used. Perfect removal of the noise due to unnecessary frequencies could be done if experiment were done for infinitely long time. Thus, FT method used by Wilhelm group (1998; 1999; 2000) requires long series of stress data measured over many cycles in order to obtain clear spectrum. Typically, they acquired about 20-50 cycles of the fundamental frequency for each sweep (Wilhelm *et al.*, 1999).

*Corresponding author: polphy@knu.ac.kr

It is reported that peaks of even harmonics are found in the FT spectrum of LAOS. The even harmonics are thought to originate from experimental insufficiencies (Onogi *et al.*, 1970). Wall slip is supposed to be the main reason for the occurrence of even harmonic (Reimers and Dealy, 1996). Graham (1995) established the occurrence of even harmonics with a bifurcation caused by wall slip. Mas and Magnin (1997) assumed the yield stress to be a reason for the occurrence of even harmonics. Wilhelm *et al.* (1998) explained the appearance of even harmonics arising from time-dependent memory effect or nonlinear elastic contribution in the system. Usually the intensity of even harmonics is as small as that of noise. It is doubtable that sometimes the occurrence of even harmonics results from imperfect cancellation of the unnecessary frequencies in numerical FT analysis.

Recently, Cho *et al.* (2005) developed a new interpretation method for LAOS by decomposing stress into elastic and viscous parts using the symmetric properties of shear stress. The method is named as "stress decomposition" (SD) in this paper. They also showed that SD is equivalent to FT from the mathematical view points. It is interesting that SD inherently excludes non integral multiples of the primary frequency. Furthermore SD method requires only a single period data, measured in a fully developed stationary condition.

We compare SD with FT from the viewpoint of numerical processing because SD is expected to be more precise than FT because it deals with only odd harmonics. We find a method to obtain the spectrum of FT from SD. The method is used to show that SD is more precise than FT. The difference between SD and FT is explained.

## 2. Interpretation methods

In an oscillatory shear flow, a sinusoidal input $\xi(t)$ with large amplitude at a frequency of $\omega$ produces a distorted wavy output $\psi(t)$ that can be decomposed into odd harmonics of sinusoidal waves in the fully developed stationary conditions, if the output satisfies following conditions:

1. The output is a sufficiently smooth function of the input and its time derivatives, so that the output can be expanded by the Taylor expansion:

$$\psi(t) = \psi\left(\xi, \frac{d\xi}{dt}, \frac{d^2\xi}{dt^2}, \ldots\right) = \psi\left(\xi, \frac{d\xi}{dt}\right) = \sum_m \sum_n a_{mn} \xi^m \left(\frac{d\xi}{dt}\right)^n \quad (1)$$

2. The output satisfies the macroscopic time-reversibility.

$$\psi(t) = \psi\left(\xi, \frac{d\xi}{dt}\right) = -\psi\left(-\xi, -\frac{d\xi}{dt}\right) \quad (2)$$

In Eq. (1), it is easy to know that only the input and its first time-derivative are necessary because the input is sinusoidal. Symmetric condition of Eq. (2) results in the sum of exponents $n+m$ must be odd integer, which explains that the output consists of only odd harmonics. It was already proved by Cho *et al.* (2005). The existence of the Taylor series of Eq. (1) is equivalent to the existence of Fourier series such that

$$\psi(t) = \sum_{k=0} [I_{2k+1}\sin(2k+1)\omega t + J_{2k+1}\cos(2k+1)\omega t] \quad (3)$$

because

$$\xi(t) = \xi_o \sin\omega t, \quad \frac{d\xi}{dt} = \omega\xi_o\cos\omega t \quad (4)$$

$$\sin^3\omega t = \frac{1}{4}(-\sin 3\omega t + 3\sin \omega t)$$
$$\sin^5\omega t = \frac{1}{16}(\sin 5\omega t - 5\sin 3\omega t + 10\sin \omega t)$$
$$\sin^7\omega t = \frac{1}{64}(-\sin 7\omega t + 7\sin 5\omega t - 21\sin 3\omega t + 35\sin \omega t)$$
$$\sin^9\omega t = \frac{1}{256}(\sin 9\omega t - 9\sin 7\omega t + 36\sin 5\omega t - 84\sin 3\omega t + 126\sin \omega t) \quad (5)$$
$$\vdots$$

and

$$\cos^3\omega t = \frac{1}{4}(\cos 3\omega t + 3\cos \omega t)$$
$$\cos^5\omega t = \frac{1}{16}(\cos 5\omega t + 5\cos 3\omega t + 10\cos \omega t)$$
$$\cos^7\omega t = \frac{1}{64}(\cos 7\omega t + 7\cos 5\omega t + 21\cos 3\omega t + 35\cos \omega t)$$
$$\cos^9\omega t = \frac{1}{256}(\sin 9\omega t + 9\cos 7\omega t + 36\cos 5\omega t + 84\cos 3\omega t + 126\cos \omega t) \quad (6)$$
$$\vdots$$

In Eq. (4) the amplitude of the input is denoted by $\xi_o$. Eqs. (5) and (6) can be found in a mathematical handbook or can be derived.

In this section, we will compare two interpretation methods of LAOS from the viewpoint of numerical process. For convenience, we take strain as input and stress as output since similar discussion may be done for the reverse case. Following notation is convenient to discuss the comparison:

$$x(t) = \gamma(t) = \gamma_o \sin \omega t, \quad y(t) = \frac{1}{\omega}\frac{d\gamma(t)}{dt} = \gamma_o \cos \omega t \quad (7)$$

where $\gamma_o$ is the amplitude of strain.

### 2.1. Fourier transform analysis

In principle, shear stress can be expressed as Fourier series in following way:

$$\sigma(t) = \sum_{k=0} K_{2k+1}\sin(2k+1)\omega t + \sum_{k=0} L_{2k+1}\cos(2k+1)\omega t \tag{8}$$

when strain is given by

$$\gamma(t) = \gamma_o \sin \omega t \tag{9}$$

In Eq. (8), the Fourier coefficients must be functions of the strain amplitude and frequency:

$$K_{2k+1} = K_{2k+1}(\gamma_o, \omega), \quad L_{2k+1} = L_{2k+1}(\gamma_o, \omega) \tag{10}$$

For the purpose of discrete FT, the shear stress with sampling acquisition interval $\Delta t$ can be represented by

$$\sigma_n = \sigma(t_n) = \sigma(n\Delta t) \tag{11}$$

and its discrete Fourier transform is given by

$$\tilde{\sigma}_n = \tilde{\sigma}(f_n) = \tilde{\sigma}\left(\frac{n}{N\Delta t}\right) = \sum_{k=0}^{N-1} \sigma_k \exp\left(-\mathbf{i}\frac{2\pi kn}{N}\right) \tag{12}$$

where $N$ is the total number of data and $\mathbf{i} = \sqrt{-1}$. Inverse Fourier transform gives

$$\sigma_n = \frac{1}{N}\sum_{k=0}^{N-1} \tilde{\sigma}_k \exp\left(\mathbf{i}\frac{2\pi nk}{N}\right) \tag{13}$$

If we denote the Fourier transform $\tilde{\sigma}_n$ as follows:

$$\tilde{\sigma}_n \equiv \tilde{\sigma}_n^{\mathrm{Re}} - \mathbf{i}\tilde{\sigma}_n^{\mathrm{Im}} \tag{14}$$

then we have

$$\sigma_n = \frac{1}{N}\sum_{k=0}^{N-1} \tilde{\sigma}_n^{\mathrm{Re}} \cos\omega_k t_n + \frac{1}{N}\sum_{k=0}^{N-1} \tilde{\sigma}_n^{\mathrm{Im}} \sin\omega_k t_n \tag{15}$$

In Eq. (15) we use the fact that shear stress is real and

$$\omega_n = \frac{2\pi n}{N\Delta t}, \quad t_n = n\Delta t \tag{16}$$

Since the primary frequency $\omega$ is given by

$$\omega = \frac{2\pi}{N\Delta t} = \omega_1 \tag{17}$$

comparison of Eq. (15) with Eq. (8) yields

$$\tilde{\sigma}_{2n}^{\mathrm{Re}} = \tilde{\sigma}_{2n}^{\mathrm{Im}} = 0 \quad \text{for} \quad n = 0,1,2,... \tag{18}$$

From Eq. (12) we know that

$$\tilde{\sigma}_n^{\mathrm{Re}} = \sum_{k=0}^{N-1} \sigma_k \cos\omega_n t_k, \quad \tilde{\sigma}_n^{\mathrm{Im}} = \sum_{k=0}^{N-1} \sigma_k \sin\omega_n t_k \tag{19}$$

Thus, Eq. (18) implies

$$\sum_{k=0}^{N-1} \sigma_k \cos 2n\omega t_k = 0, \quad \sum_{k=0}^{N-1} \sigma_k \sin 2n\omega t_k = 0 \tag{20}$$

However, measured shear stress includes some errors and Eq. (20) real and imaginary parts of the Fourier transform of shear stress for even integer are not exactly zero. Thus, we can rewrite $\sigma_k$ as follows:

$$\sigma_k = S_k + \varepsilon_k \tag{21}$$

where

$$\sum_{k=0}^{N-1} S_k \cos 2n\omega t_k = 0, \quad \sum_{k=0}^{N-1} S_k \sin 2n\omega t_k = 0 \tag{22}$$

and

$$\sum_{k=0}^{N-1} \varepsilon_k \cos 2n\omega t_k \neq 0, \quad \sum_{k=0}^{N-1} \varepsilon_k \sin 2n\omega t_k \neq 0 . \tag{23}$$

It is noteworthy that the first part of the right hand sides of Eq. (8) is in-phase with strain and the second part is in-phase with strain rate. Although the plot of stress versus strain (or strain rate) forms a loop, the plot of the first part versus strain and the plot of the second part versus strain rate do not form any loop. These plots of no loop indicate functions. Thus, it is clear that the first part is elastic stress and the second part is viscous stress. The decomposition of stress by FT can be done by following procedures:

[1] Determine the Fourier coefficients $\tilde{\sigma}_k^{\mathrm{Re}}$ and $\tilde{\sigma}_k^{\mathrm{Im}}$.

[2] Construct Eq. (8) by use of $\tilde{\sigma}_k^{\mathrm{Re}}$ and $\tilde{\sigma}_k^{\mathrm{Im}}$ of only odd harmonics.

Wilhelm *et al.* (1998; 1999; 2000) used

$$I_{2k+1} \equiv \frac{\sqrt{(\tilde{\sigma}_{2k+1}^{\mathrm{Re}})^2 + (\tilde{\sigma}_{2k+1}^{\mathrm{Im}})^2}}{N} \tag{24}$$

as a measure of nonlinearity of shear stress instead of each $\tilde{\sigma}_k^{\mathrm{Re}}$ and $\tilde{\sigma}_k^{\mathrm{Im}}$. It is similar to the linear viscoelastic analysis that uses $G^*(\omega) \equiv \sqrt{[G'(\omega)]^2 + [G''(\omega)]^2}$ instead of the storage and the loss moduli. Thus, they used parts of information from a nonlinear experiment instead of whole information.

### 2.2. Stress decomposition

From the help of Eqs. (1), (2) and (7), we can express the shear stress of LAOS as follows:

$$\sigma(t) = \sum_m \sum_n a_{nm}(\omega) x^m y^n \tag{25}$$

Note that $m + n$ must be an odd integer in order to satisfy the symmetric condition of shear stress Eq.(2). Since the strain amplitude is given by

$$\gamma_o^2 = x^2(t) + y^2(t) \tag{26}$$

From the help of Eq. (26), we can rewrite even powers of $x$ or $y$ as follows:

$$x^{2k}(t) = [\gamma_o^2 - y^2(t)]^k, \quad y^{2k}(t) = [\gamma_o^2 - x^2(t)]^k \tag{27}$$

Thus, we can rewrite Eq. (25) by use of Eq. (27) as follows:

$$\sigma(t) = \sum_{k=0} A_{2k+1}(\omega,\gamma_o)x^{2k+1}(t) + \sum_{k=0} B_{2k+1}(\omega,\gamma_o)y^{2k+1}(t) \quad (28)$$

A simple but long mathematical manipulation gives the relation between the coefficients $a_{mn}(\omega) \rightarrow A_{2k+1}(\omega, \gamma_o)$ and $a_{mn}(\omega) \rightarrow B_{2k+1}(\omega, \gamma_o)$. Eqs. (5) and (6) convert Eq. (28) to Eq. (8). It is noteworthy that the first and the second parts of Eq. (28) are, respectively, equivalent to the corresponding parts of Eq. (8). Thus, we can denote elastic stress σ' and viscous stress σ" as follows [Cho *et al.* (2005)]:

$$\sigma'(t) \equiv \sum_{k=0} A_{2k+1}(\omega,\gamma_o)x^{2k+1}(t), \quad \sigma''(t) \equiv \sum_{k=0} B_{2k+1}(\omega,\gamma_o)y^{2k+1}(t) \quad (29)$$

Eq. (29) shows that the elastic stress is even for $y$ and odd for $x$ and the viscous stress is even for $x$ and odd for $y$. Thus the two stresses can be rewritten by

$$\sigma' = \sigma'(x,y), \quad \sigma'' = \sigma''(x,y) \quad (30)$$

It is unique decomposition that

$$\sigma(x,y) = \frac{\sigma(x,y)-\sigma(-x,y)}{2} + \frac{\sigma(x,y)+\sigma(-x,y)}{2} \quad (31)$$

Due to time-reversibility of shear stress in Eq. (2), it is obvious that the first part of the right hand side of Eq. (31) is odd for $x$ and even for $y$ and the second part is odd for $y$ and even for $x$. The uniqueness of the decomposition Eq. (31) leads that the first part is elastic stress σ' and the second part is viscous stress σ":

$$\sigma'(x,y) = \frac{\sigma(x,y)-\sigma(-x,y)}{2}, \quad \sigma''(x,y) = \frac{\sigma(x,y)+\sigma(-x,y)}{2} \quad (32)$$

Since the strain rate over frequency, $y$ are given by differentiation of strain $x$, we have three columns of data, $x$, $y$ and σ as functions of time. For a fixed row of data ($x$, $y$, σ ($x$,$y$)), we can find a row of data ($-x$, $y$, σ ($-x$,$y$)). Then we can obtain elastic and viscous stresses at ($x$, $y$) by use of Eq. (32). Repeating this procedures for all rows of data, we finally have five columns of data: $x$, $y$, σ, σ', and σ" as functions of time. It is a process of searching data. As mentioned above, the plot of elastic stress versus strain $x$, and the plot of viscous stress versus strain rate or $y$ do not form any loop. Thus, we can determine the coefficients $A_{2k+1}$ and $B_{2k+1}$ by use of regression at a given amplitude of strain.

Once we determine the coefficients $A_{2k+1}$ and $B_{2k+1}$, we can determine the Fourier coefficients $K_{2k+1}$ and $L_{2k+1}$ of Eq. (8). Since ninth order of polynomial in Eq. (29) is sufficient to describe most experimental data well, for the truncated series of ninth order, we have

$$K_1 = A_1\gamma_o + \frac{3}{4}A_3\gamma_o^3 + \frac{10}{16}A_5\gamma_o^5 + \frac{35}{64}A_7\gamma_o^7 + \frac{126}{256}A_9\gamma_o^9$$
$$L_1 = B_1\gamma_o + \frac{3}{4}B_3\gamma_o^3 + \frac{10}{16}B_5\gamma_o^5 + \frac{35}{64}B_7\gamma_o^7 + \frac{126}{256}B_9\gamma_o^9 \quad (33a)$$

$$K_3 = -\frac{1}{4}A_3\gamma_o^3 - \frac{5}{16}A_5\gamma_o^5 - \frac{21}{64}A_7\gamma_o^7 - \frac{84}{256}A_9\gamma_o^9$$
$$L_3 = \frac{1}{4}B_3\gamma_o^3 + \frac{5}{16}B_5\gamma_o^5 + \frac{21}{64}B_7\gamma_o^7 + \frac{84}{256}B_9\gamma_o^9 \quad (33b)$$

$$K_5 = \frac{1}{16}A_5\gamma_o^5 + \frac{7}{64}A_7\gamma_o^7 + \frac{36}{256}A_9\gamma_o^9$$
$$L_5 = \frac{1}{16}B_5\gamma_o^5 + \frac{7}{64}B_7\gamma_o^7 + \frac{36}{256}B_9\gamma_o^9 \quad (33c)$$

$$K_7 = -\frac{1}{64}A_7\gamma_o^7 - \frac{9}{256}A_9\gamma_o^9$$
$$L_7 = \frac{1}{64}B_7\gamma_o^7 + \frac{9}{256}B_9\gamma_o^9 \quad (33d)$$

$$K_9 = \frac{1}{256}A_9\gamma_o^9, \quad L_9 = \frac{1}{256}B_9\gamma_o^9 \quad (33e)$$

Thus, SD provides the same results as FT without giving unnecessary frequencies. Furthermore, SD decomposes stress first and determines coefficients $A_{2k+1}$ and $B_{2k+1}$, while FT does in the reverse way. Because SD decompose stress first, one may find an empirical model describing elastic and viscous stress as functions of $x$ and $y$ in close form, not in polynomial.

In order to investigate dependence of $A_{2k+1}$ and $B_{2k+1}$ on strain amplitude, Eq. (28) can be rewritten as follows:

$$\sigma(t) = \sum_{k=0} \gamma_0^{2k+1}A_{2k+1}(\omega,\gamma_o)\sin^{2k+1}\omega t$$
$$+ \sum_{k=0} \gamma_0^{2k+1}B_{2k+1}(\omega,\gamma_o)\cos^{2k+1}\omega t \quad (34)$$

Since absolute values of powers of trigonometric functions lie between −1 and 1, requirement of convergence of infinite series may result in

$$A_{2k+1} \sim \frac{1}{\gamma_o^n}, \quad B_{2k+1} \sim \frac{1}{\gamma_o^n} \text{ for large } k \quad (35)$$

where $n \geq 2k+1$. Otherwise, the infinite series may diverse at large strain amplitude.

## 3. Discussion

### 3.1. Analysis for simulated data

It is interesting to compare precision of FT with that of SD by generating data from the following equation:

$$\sigma(t) = K_1 \sin \omega t + L_1 \cos \omega t + K_3 \sin 3\omega t + L_3 \cos 3\omega t \quad (36)$$

Since the calculated data from Eq. (36) do not contain any sinusoidal wave of frequency different from ω and 3ω, we can compare the precision of both the methods and the effect of unnecessary frequencies on both the results. To compare the values of $K_{2n+1}$ and $L_{2n+1}$ in Eq. (36) determined by the two methods, Eq. (36) was rewritten in the form of SD as follows:

$$\sigma(t) = A_1\gamma_o \sin\omega t + A_3\gamma_o^3 \sin^3\omega t + B_1\gamma_o \cos\omega t + B_3\gamma_o^3 \cos^3\omega t \quad (37)$$

The coefficients $K_{2n+1}$ and $L_{2n+1}$ is related with the coefficients $A_{2n+1}$ and $B_{2n+1}$ of SD. The highest harmonics in Eq. (36) is only 3rd harmonic. Thus, the relation is

$$K_1 = A_1\gamma_o + \frac{3}{4}A_3\gamma_o^3,\quad L_1 = B_1\gamma_o + \frac{3}{4}B_3\gamma_o^3$$
$$K_3 = -\frac{A_3\gamma_o^3}{4},\quad L_3 = \frac{B_3\gamma_o^3}{4} \quad (38)$$

We generated stress as a function of time with

$$\Delta t = \frac{2\pi}{100},\quad T = 2\pi N_p$$
$$K_1 = 1.00000\times10^0,\quad L_1 = 5.00000\times10^{-1}$$
$$K_3 = 1.00000\times10^{-1},\quad L_3 = 5.00000\times10^{-2} \quad (39)$$

where $\Delta t$ is the time step, $T$ is the upper limit of time, $N_p$ is an integer that obtained by dividing $T$ by the period $2\pi/\omega$. It is necessary to test whether FT precisely determines the values of $K_{2n+1}$ and $L_{2n+1}$ from the data generated from Eq. (36) and to compare them with those of $K_{2n+1}$ and $L_{2n+1}$ determined by SD. Table 1 summarizes the coefficients obtained by FT and SD. SD decomposes the stress generated from Eq. (36) and determines the coefficients of $A_{2n+1}$ and $B_{2n+1}$ by use of regression. With the help of Eq. (38), we can determine the coefficients $K_{2n+1}$ and $L_{2n+1}$. Because of the symmetry of discrete Fourier Transform, we know that

$$K_{2n+1} = \frac{2}{N}\tilde{\sigma}^{\mathrm{Im}}_{2n+1},\quad L_{2n+1} = \frac{2}{N}\tilde{\sigma}^{\mathrm{Re}}_{2n+1} \quad (40)$$

It is wonderful that SD seems to involve no errors in determination of the coefficients $K_{2n+1}$ and $L_{2n+1}$ irrespective of the amount of data (viz. $N_p$) while FT suffer from some errors which decrease as $N_p$ increases in case of $K_3$ and $L_3$ (Table 1). The errors of FT may be originated from truncation errors in calculation of trigonometric functions in Eq. (19) and the unnecessarily involved frequencies which is inherent in FT analysis. Results of Table 1 imply that the precision of FT analysis increases with decreasing sampling time $\Delta t$ and increasing the length of time series $T$. Thus large number of data with high sampling rate is necessary to obtain reliable and precise FT results, while SD needs only a single period data in a fully developed stationary condition.

### 3.2. Analysis for the data from constitutive model

Now, we apply SD and FT to analysis of LAOS data generated from a nonlinear viscoelastic constitutive equation. The Phan-Thien and Tanner model is chosen:

$$\lambda_k\left(\frac{d\mathbf{C}_k}{dt} - \mathbf{L}\cdot\mathbf{C}_k - \mathbf{C}_k\cdot\mathbf{L}^T\right) + \mathbf{S}(\mathbf{C}_k) = \mathbf{0} \quad (41a)$$

$$\mathbf{S}(\mathbf{C}_k) = \phi(I_k)(\mathbf{C}_k - \mathbf{I}) \quad (41b)$$

$$\phi(I_k) = \exp[-\varepsilon(I_k - 3)] \quad (41c)$$

$$I_k = \mathrm{tr}(\mathbf{C}_k) \quad (41d)$$

$$\mathbf{T} = \sum_{k=} G_k(\mathbf{C}_k - \mathbf{I}) \quad (41e)$$

where $\mathbf{L}$ is the velocity gradient, $\mathbf{C}_k$ is the conformation tensor of $k$th mode, $\varepsilon$ is the nonlinear parameter of the model and the linear viscoelastic parameters $\lambda_k$ and $G_k$ can be determined by relaxation time spectra. The relaxation time spectra used in this analysis is shown in Table 2. We used the values of parameters in this calculation: $\varepsilon = 0.3$, $T = 50$, $\omega_1 = 1$ rad/sec, and $\Delta t = 0.025$.

Fig. 1 shows the wave form of shear stress as a function of time with varying strain amplitude. As strain amplitude exceeds $\gamma_o = 3$, the wave form of stress becomes distorted significantly.

Fig. 2 shows the spectrum of FT $I(\omega_k)$, $K(\omega)$ and $L(\omega)$ as functions of angular frequency. The spectrum obtained from a long series of stationary data (six periods). The spectrum shows significant peaks at odd harmonics. Since stress data obtained from the calculation of Eq. (41) has negligible errors during numerical procedure, the spectrum looks like noise-free.

**Table 1.** The values of the coefficients $K_{2n+1}$ and $L_{2n+1}$ determined by FT and SD for the data generated by Eq. (36)

| $N_p$ | Fourier Transform | | | | Stress Decomposition | | | |
|---|---|---|---|---|---|---|---|---|
| | $K_1$ | $K_3$ | $L_1$ | $L_3$ | $K_1$ | $K_3$ | $L_1$ | $L_3$ |
| 1 | 1.00915 | 0.11108 | 0.47052 | 0.05410 | 1.00000 | 0.10000 | 0.50000 | 0.05000 |
| 2 | 1.01210 | 0.10762 | 0.46939 | 0.04567 | 1.00000 | 0.10000 | 0.50000 | 0.05000 |
| 5 | 1.01387 | 0.10552 | 0.46871 | 0.04245 | 1.00000 | 0.10000 | 0.50000 | 0.05000 |
| 10 | 1.01446 | 0.10481 | 0.46849 | 0.04138 | 1.00000 | 0.10000 | 0.50000 | 0.05000 |

**Table 2.** Relaxation time spectra

| $\lambda_k$ (sec) | 500 | 200 | 50 | 10 | 2 | 0.5 | 0.1 |
|---|---|---|---|---|---|---|---|
| $G_k$ (Pa) | 61.7 | 600 | 2,970 | 14,300 | 29,600 | 8,590 | 88,900 |

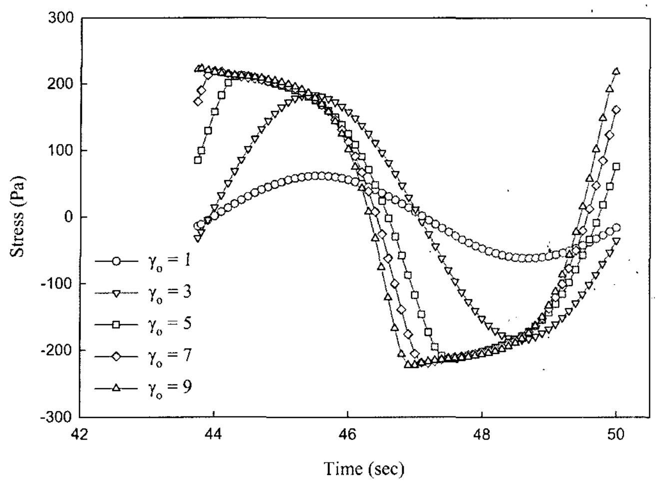


**Fig. 1.** Stress of the Phan-Thien and Tanner model as a function of time. The calculated data used relaxation time spectrum shown in Table 3. The values of parameters of the model are written in the text.

Reading the heights of the peaks of odd harmonics, we can plot the reduced intensity of odd harmonics $I_{2k+1}/I_1$ versus strain amplitude, as Wilhelm's group did. SD can also determine the relative intensity of FT through Eq. (33). Fig. 3 compares the results of SD and FT. The solid symbols denote the intensities determined by FT and the open symbols denote those determined by SD. The values from both methods agrees well when the relative intensity is larger than 0.01. If the relative intensity becomes less than 0.01, there appears considerable difference between the values of the two methods. As for $I_3/I_1$, the relative spectrum determined by SD shows that a smooth functional relation between $I_3/I_1$ and strain amplitude keeps valid even at low strain amplitudes. However, those determined by FT shows that the smooth relation breaks at low strain amplitude. The difference between the two spectrums seems originated from numerical errors of FT due to discretization as shown in the previous section.

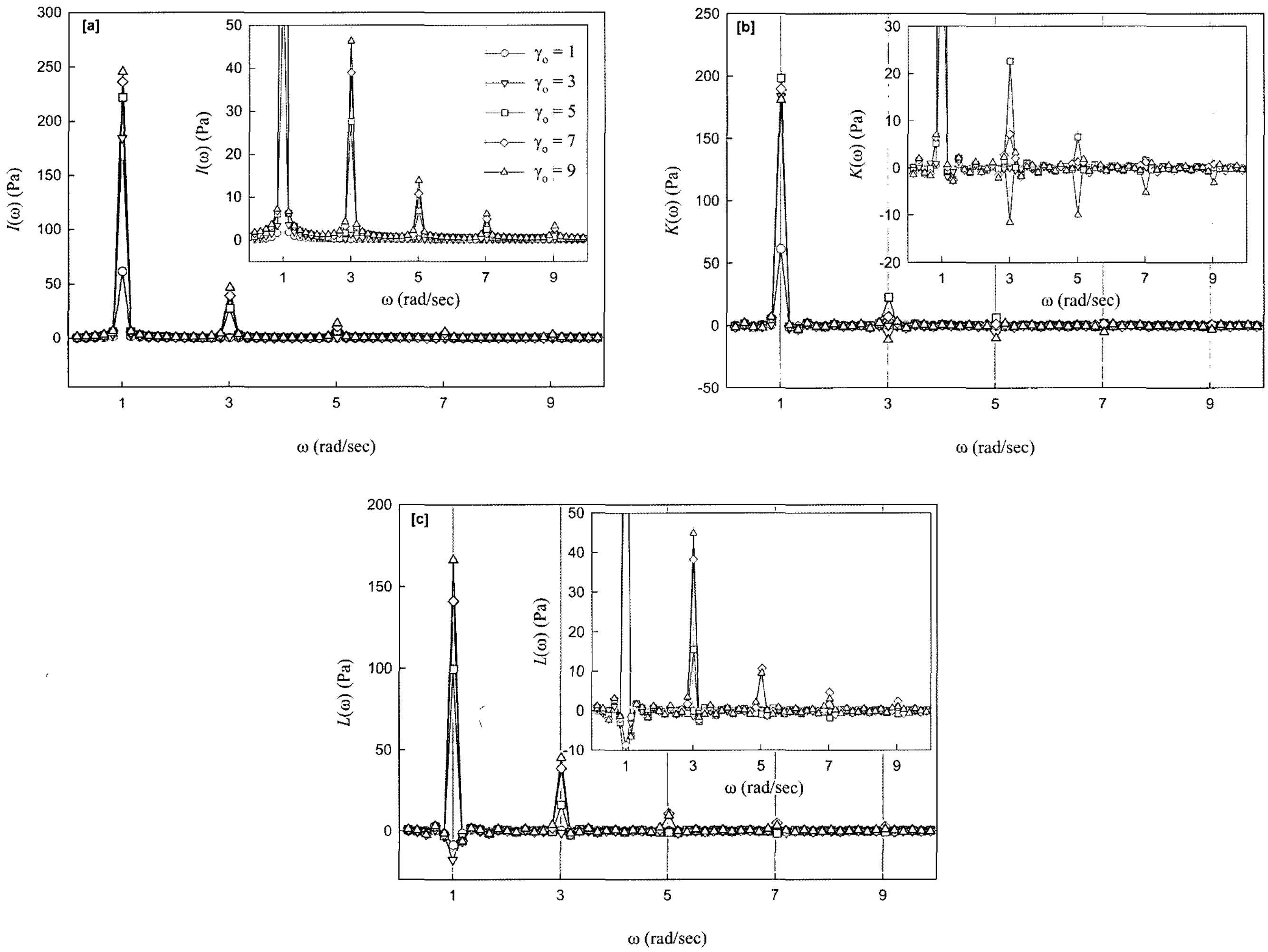


**Fig. 2.** Results of Fourier transform. [a], [b] and [c] are, respectively, $I$, $K$ and $L$ as functions of frequency ω. The discrete FT was done by use of Eqs. (19), (24) and (40).

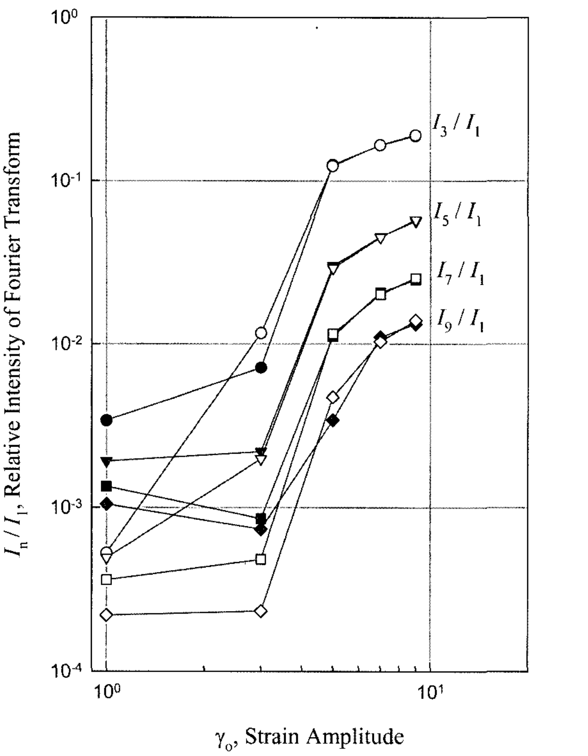


**Fig. 3.** Comparison of relative intensities of Fourier transform as functions of strain amplitude. The intensities are determined by FT (filled symbols) and SD (open symbols).

Table 3 shows the coefficients of FT, $K_{2n+1}$ and $L_{2n+1}$ determined by FT and SD as well as the coefficients of SD $A_{2n+1}$ and $B_{2n+1}$. The values in the table were determined under the assumption that stress data do not contain higher than ninth order harmonics. The determination of the FT coefficients $K_{2n+1}$ and $L_{2n+1}$ by SD method was done by use of Eq. (33). The values of the coefficients $K_{2n+1}$ and $L_{2n+1}$ or $A_{2n+1}$ and $B_{2n+1}$ allows construction of stress data. Fig. 4 shows the comparison of the stress data calculated from Eq. (41) with reconstructed stress data from the values of coefficients of SD and FT. As shown in the figure, the reconstructed stress by FT shows phase-shift to the right in time axis while that of SD agrees well with the original data. It is noteworthy that the analysis of SD was done for a set of stress data of a single period while FT analysis was done for about 6-period data. Fig. 5 shows the plot of the FT coefficients $K_{2n+1}$ and $L_{2n+1}$ determined by SD method versus the FT coefficients $K_{2n+1}$ and $L_{2n+1}$ determined by FT. As expected, the two methods have good correlation.

## 4. Conclusion

We compared precision of FT and SD from the view points of numerical scheme. Since SD does not involve unnecessary frequencies, it shows higher precision than FT

**Table 3.** Coefficients of FT and SD determined from the stress data generated by Eq. (41) at various strain amplitudes.

| | | Strain Amplitude $\gamma_o$ | | | | |
|---|---|---|---|---|---|---|
| | | 1 | 3 | 5 | 7 | 9 |
| FT method | $K_1$ | 6.11E+1 | 1.84E+2 | 1.98E+2 | 1.89E+2 | 1.81E+2 |
| | $K_3$ | 2.09E−1 | 4.12E−2 | 2.26E+1 | 7.17E+0 | −1.15E+1 |
| | $K_5$ | 1.18E−1 | 3.49E−1 | 6.59E+0 | 1.28E+0 | −1.00E+1 |
| | $K_7$ | 8.29E−2 | 1.55E−1 | 1.73E+0 | 1.31E+0 | −5.18E+0 |
| | $K_9$ | 6.45E−2 | 1.36E−1 | 8.60E−2 | 8.74E−1 | −3.09E+0 |
| | $L_1$ | −8.72E+0 | −1.79E+1 | 9.94E+1 | 1.41E+2 | 1.66E+2 |
| | $L_3$ | −9.14E−3 | −1.32E+0 | 1.58E+1 | 3.83E+1 | 4.49E+1 |
| | $L_5$ | 1.04E−3 | 2.06E−1 | −8.93E−1 | 1.06E+1 | 9.54E+0 |
| | $L_7$ | 2.75E−3 | −2.94E−2 | −1.75E+0 | 4.70E+0 | 3.09E+0 |
| | $L_9$ | 3.54E−3 | 7.39E−3 | −7.52E−1 | 2.45E+0 | 9.92E−1 |
| SD method | $K_1$ | 6.17E+1 | 1.83E+2 | 1.82E+2 | 1.67E+2 | 1.54E+2 |
| | $K_3$ | −8.51E−4 | 3.88E−1 | 1.35E+1 | −1.04E+1 | −3.04E+1 |
| | $K_5$ | −1.03E−3 | −2.31E−1 | 5.52E+0 | −6.37E+0 | −1.42E+1 |
| | $K_7$ | −9.86E−4 | 6:10E−2 | 2.55E+0 | −3.32E+0 | −5.26E+0 |
| | $K_9$ | −7.43E−4 | 3.94E−2 | 9.55E−1 | −2.03E+0 | −1.44E+0 |
| | $L_1$ | 2.66E−1 | 1.38E+1 | 1.28E+2 | 1.68E+2 | 1.92E+2 |
| | $L_3$ | 3.25E−2 | −2.11E+0 | 2.37E+1 | 3.78E+1 | 3.56E+1 |
| | $L_5$ | 3.04E−2 | 2.80E−1 | 3.31E+0 | 8.52E+0 | −1.83E−1 |
| | $L_7$ | 2.23E−2 | −6.45E−2 | 1.52E−1 | 3.38E+0 | −3.32E+0 |
| | $L_9$ | 1.36E−2 | −1.71E−2 | −4.44E−1 | 1.35E+0 | −3.11E+0 |
| | $A_1$ | 6.17E+1 | 6.14E+1 | 5.52E+1 | 8.84E+0 | −6.37E+0 |
| | $A_3$ | 1.68E−1 | −1.88E−1 | −3.37E+0 | 1.75E+0 | 1.20E+0 |
| | $A_5$ | −4.48E−1 | 8.30E−2 | 2.52E−1 | −8.04E−2 | −2.43E−2 |
| | $A_7$ | 4.91E−1 | −1.22E−2 | −9.13E−3 | 1.68E−3 | 2.43E−4 |
| | $A_9$ | −1.90E−1 | 5.13E−4 | 1.25E−4 | −1.29E−5 | −9.48E−7 |
| | $B_1$ | 2.86E−1 | 7.27E+0 | 1.36E+1 | 1.23E+1 | 8.80E+0 |
| | $B_3$ | −8.56E−1 | −5.78E−1 | 7.25E−1 | 2.21E−2 | 4.57E−1 |
| | $B_5$ | 3.85E+0 | 1.78E−2 | −4.99E−2 | 2.04E−2 | −1.65E−2 |
| | $B_7$ | −6.39E+0 | 2.61E−3 | 3.40E−3 | −6.84E−4 | 3.30E−4 |
| | $B_9$ | 3.47E+0 | −2.22E−4 | −5.82E−5 | 8.59E−6 | −2.05E−6 |

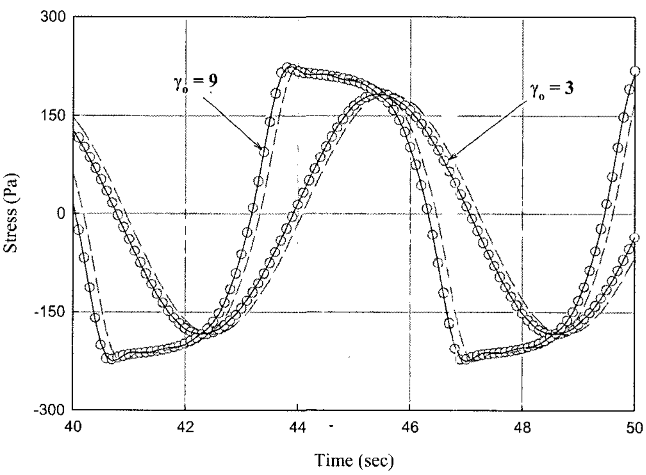


**Fig. 4.** Comparison of wave forms of shear stress, which are reconstructed from coefficients of FT and SD. The values of the coefficient are determined through the two methods FT and SD by using the data of Fig. 1.

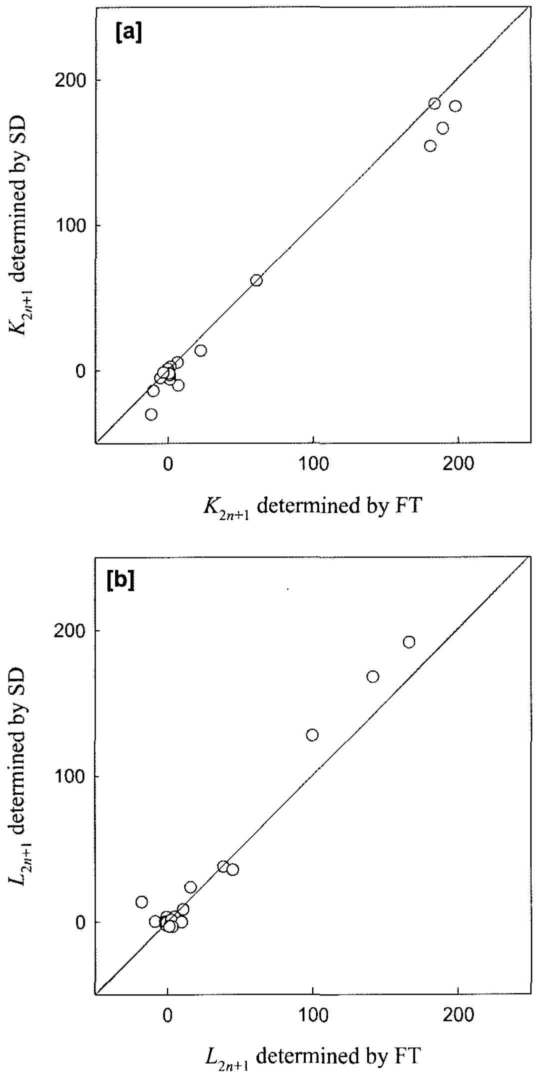


**Fig. 5.** Comparison of FT coefficients calculated by the two methods, FT and SD.

which suffers from the effect of unnecessary frequencies which originates from discretization. The most important advantage of SD compared with FT is that data of just a single period are sufficient for SD under fully developed stationary state, while FT requires high rate of sampling and long series of data of many cycles in order to achieve sufficient precision. Since SD decompose shear stress into elastic and viscous parts without determination of coefficients, it is possible to model the elastic and viscous stresses in a closed form. However, FT can decompose shear stress after determination of coefficients which may suffer from doomed errors.

## Acknowledgment

This research was supported by Kyungpook National University Research Fund, 2005.

## References

Cho, K.S., K. Hyun, K.H. Ahn and S.J. Lee, 2005, A geometrical interpretation of large amplitude oscillatory shear response, *J. Rheol.* **49**, 747-758.

Dusschoten, D.V. and M. Wilhelm, 2001, Increased torque transducer sensitivity via oversampling, *Rheol. Acta* **40**, 395-399.

Giacomine, A.J. and J.M. Dealy, 1993, Large-amplitude oscillatory shear," in *Techniques in Rheological Measurements* edited A. A. Collyer (Chapman & Hall, London) Chapter 4.

Graham, M.D., 1995, Wall slip and the nonlinear dynamics of large amplitude oscillatory shear flows, *J. Rheol.* **39**, 697.

Krieger, I.M. and T.F. Niu, 1973, A rheometer for oscillatory studies of nonlinear fluids, *Rheol. Acta* **12**, 567-571.

Kallus, S., N. Willenbacher, S. Kirsch, D. Distler, T. Neidhofer, M. Wilhelm and H.W. Spiess, 2001, Characterization of polymer dispersions by Fourier transform rheology, *Rheol. Acta* **40**, 552-559.

Mas, R. and A. Magnin, 1997, Experimental validation of steady shear and dynamic viscosity relation for yield stress fluids, *Rheol. Acta* **36**, 49.

Onogi, S., T. Masuda and T. Matsumoto, 1970, Nonlinear behavior of viscoelastic materials. I: Disperse systems of polystyrene solution and carbon black, *Trans. Soc. Rheol.* **14**, 275.

Philippoff, W., 1966, Vibrational measurements with large amplitudes, *Trans. Soc. Rheol.* **10**, 317.

Reimers, M.J. and J.M. Dealy, 1996, Sliding plate rheometer studies of concentrated polystyrene solutions: Large amplitude oscillatory shear of a very high molecular weight polymer in diethyl phthalate, *J. Rheol.* **40**, 167.

Wilhelm, M., D. Maring and H.W. Spiess, 1998, Fourier-transform rheology, *Rheol. Acta* **37**, 399-405.

Wilhelm, M., P. Reinheimer and M. Ortseifer, 1999, High sensitivity Fourier-transform rheology, *Rheol. Acta* **38**, 349-356 (1999).

Wilhelm, M., P. Reinheimer and M. Ortseifer, T. Neidhöfer and H.W. Spiess, 2000, The crossover between linear and nonlinear mechanical behaviour in polymer solutions as detected by Fourier-transform rheology, *Rheol. Acta* **39**, 241.